Available online at www.sciencedirect.com
ScienceDirect
Dyes and Pigments 79 (2008) 69–75
DYES and PIGMENTS
www.elsevier.com/locate/dyepig

Structural and computational studies of azo dyes in the hydrazone form having the same pyridine-2,6-dione component (II): C.I. Disperse Yellow 119 and C.I. Disperse Yellow 211

Wei Huang*

State Key Laboratory of Coordination Chemistry, Coordination Chemistry Institute, Nanjing University–Jinchuan Group Ltd. Joint Laboratory of Metal Chemistry, School of Chemistry and Chemical Engineering, Nanjing University, Nanjing 210093, PR China

Received 6 August 2007; received in revised form 15 January 2008; accepted 15 January 2008
Available online 25 January 2008

Abstract

The molecular and crystal structures of two yellow, azo disperse dyes having the same pyridine-1-ethyl-3-cyano-4-methyl-2,6-dione backbone, namely C.I. Disperse Yellow 119 and C.I. Disperse Yellow 211 were studied. Both dyes crystallize in the hydrazone form both at 291 and 120 K, with hydrogen bonding and π–π stacking interactions playing important roles in determining the packing frameworks; mean interlayer separations of 3.002(3) and 3.316(6) Å, respectively, were obtained. Theoretical calculations were undertaken to compare the energy differences between the single-crystal and the energy-minimized structures of the compounds as well as those between the pyridine-2,6-dione and the 2-hydroxy-6-pyridone isomers.

Keywords: Azo dyes; C.I. Disperse Yellow; Tautomerism; Supramolecular frameworks

1. Introduction

Disperse dyes are a family of non-ionic aromatic compounds, scarcely soluble in water but soluble in organic solvents. The majority of them are azo and anthraquinone dyes and several series of C.I. Disperse Yellow, Red, Orange, Purple, Blue, Green, Brown, and Black are commercially available. Nowadays, azo dyes of C.I. Disperse Yellow series and their derivatives are widely used in the dyestuff industry.

It is known that azo dyes synthesized from the pyridine-2,6-dione based coupling components have two types of enantiotropic isomers, i.e. the 2-hydroxy-6-pyridone form and the pyridine-2,6-dione form. A practical way to assign the conformation of this type of azo dyes is the X-ray single-crystal structural diffraction determination where the information on the molecules, such as the way of atoms' connection, geometric conformation, bond lengths and angles, dihedral angles between planes and so on, can be obtained. However, the structural reports on this type of azo dyes are few, and in most cases (such as in Chemical Abstracts) they are named as the 2-hydroxy-6-pyridone forms which are different from their solid structures revealed by the X-ray single-crystal diffraction method.

On considering numerous publications which have focused on the industrial applications such as dye fixing [1–6], pasting and dispersing [7,8], printing [9,10] and so on, the structural characterizations on the intermolecular and intramolecular interactions in supramolecular level and the computational studies on conformation originated from the isomerization/tautomerism or the stereochemistry of molecules are rarely involved. We extend our work in this paper by investigating two new C.I. Disperse Yellow structures having pyridine-2,6-dione coupling component in the hydrazone form, namely C.I. Disperse Yellow 119 and C.I. Disperse Yellow 211 (Scheme 1), together with systematic computational studies for four azo dyes (C.I. Disperse Yellow 114 [11], 119, 126 [12], 211) that have been structurally characterized by our

* Tel.: +86 25 83686526; fax: +86 25 83314502.
E-mail address: whuang@nju.edu.cn

0143-7208/$ - see front matter © 2008 Elsevier Ltd. All rights reserved.
doi:10.1016/j.dyepig.2008.01.007

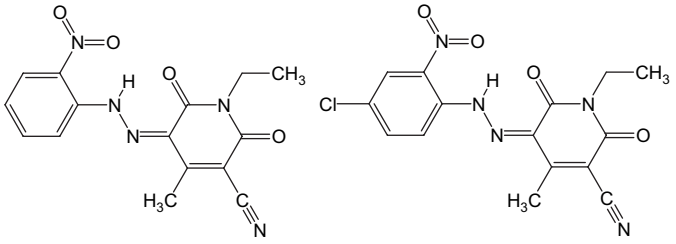

C.I. Disperse Yellow 119 (**1**) C.I. Disperse Yellow 211 (**2**)

Scheme 1. Molecular structures of C.I. Disperse Yellow 119 (**1**) and C.I. Disperse Yellow 211 (**2**) in the hydrazone form.

group, namely, the energy differences between the single-crystal and energy-minimized structures and those between the energy-minimized pyridine-2,6-dione and 2-hydroxy-6-pyridone isomers.

2. Experimental section

2.1. Materials and measurements

C.I. Disperse Yellow 119 and C.I. Disperse Yellow 211 are commercially available and were used as received for growing single crystals. All other solvents and reagents were of analytical grade and used without further purification. Single-crystal samples of C.I. Disperse Yellow 119 (**1**) and C.I. Disperse Yellow 211 (**2**) suitable for X-ray diffraction measurement were grown from the mixed solution of acetone/methanol and acetone/ethanol, respectively, in the same ratio of 1:2 (v/v) by slow evaporation in air at room temperature.

2.2. X-ray data collection and solution

Single-crystal samples of **1** and **2·CH$_3$COCH$_3$** were glue-covered and mounted on glass fibers and used for data collection on a Bruker SMART 1K CCD area detector at 291(2) and 120(2) K using graphite mono-chromated Mo Kα radiation ($\lambda = 0.71073$ Å). The collected data were reduced by using the program SAINT [13] and empirical absorption corrections were done by using the SADABS [14] program. The crystal systems were determined by Laue symmetry and the space groups were assigned on the basis of systematic absences using XPREP, and then the structures were solved by direct method and refined by least-squares method. All non-hydrogen atoms were refined on F^2 by full-matrix least-squares procedure using anisotropic displacement parameters. Hydrogen atoms were inserted in the calculated positions assigned fixed isotropic thermal parameters at 1.2 times the equivalent isotropic U of the atoms to which they are attached (1.5 times for the methyl groups) and allowed to ride on their respective parent atoms. One set of the *N*-substituted ethyl group in **2·CH$_3$COCH$_3$** is disordered over two positions, with site occupancy factors of 0.37(2) and 0.63(2) where the asymmetric unit of **2·CH$_3$COCH$_3$** contains two crystallographically independent molecules. All calculations were carried out on a PC computer with the SHELXTL PC program package [15] and molecular graphics were drawn by using XP and ChemDraw software. Details of the data collection and refinement results for compounds **1** and **2·CH$_3$COCH$_3$** are listed in Table 1, while selected bond distances and bond angles are given in Table 2.

3. Results and discussion

3.1. Structural elucidation of *1* and *2·CH$_3$COCH$_3$*

The molecular structures of **1** and **2·CH$_3$COCH$_3$** with atom-numbering scheme are shown in Figs. 1 and 2, respectively. The X-ray crystal structural analyses reveal that **1** crystallizes in the orthorhombic *Pbca* space group and one C.I. Disperse Yellow 119 molecule is included in the asymmetric unit without the presence of any solvent molecule. In contrast, **2·CH$_3$COCH$_3$** crystallizes in the monoclinic $P2_1/c$ space group exhibiting lower crystallographic symmetry, and two sets of molecules are found in the asymmetric unit where two lattice acetone solvent molecules are encapsulated. All the non-hydrogen atoms except one carbon atom of the *N*-substituted ethyl group are essentially coplanar in **1** and **2·CH$_3$COCH$_3$**. Like previously reported four structures [11,12,16,17] with the same backbone but different coupling

Table 1
Crystal data and final structural refinement results for azo dyes **1** and **2·CH$_3$COCH$_3$**

Compound	**1**	**2·CH$_3$COCH$_3$**
Empirical formula	$C_{15}H_{13}N_5O_4$	$C_{18}H_{18}ClN_5O_5$
Formula weight	327.30	419.82
T (K)	120(2)	291(2)
Crystal system	Orthorhombic	Monoclinic
Space group	*Pbca* (No. 61)	$P2_1/c$ (No. 14)
a (Å)	14.283(3)	10.148(1)
b (Å)	7.589(2)	21.518(2)
c (Å)	26.874(6)	18.498(2)
α (°)	90	90
β (°)	90	93.163(3)
γ (°)	90	90
V/Å^3	2912.8(11)	4033.0(7)
Crystal size/mm	0.10 × 0.15 × 0.35	0.10 × 0.20 × 0.25
Z	8	8
D_c (Mg m^{-3})	1.493	1.383
μ (Mo Kα) (mm^{-1})	0.112	0.229
F(000)	1360	1744
Absorption correction	Multi-scan	Multi-scan
Data collected/unique	13,594/2552	19,899/7077
Limiting indices	$-16 \le h \le 16$	$-12 \le h \le 12$
	$-9 \le k \le 8$	$-25 \le k \le 18$
	$-31 \le l \le 25$	$-19 \le l \le 21$
Parameter	219	549
Max./min. transmission	0.989/0.962	0.977/0.945
$R1$, $wR2$ ($I > 2\sigma(I)$)	$R1 = 0.0458$	$R1 = 0.0741$
	$wR2 = 0.0838$	$wR2 = 0.1463$
$R1$, $wR2$ (all data)	$R1 = 0.0794$	$R1 = 0.1743$
	$wR2 = 0.1911$	$wR2 = 0.1827$
Goodness of fit on F^2	0.849	0.959
Δ (e Å^{-3}) (max, min)	0.229/−0.279	0.314/−0.213

$R1 = \Sigma||Fo| - |Fc||/\Sigma|Fo|$, $wR2 = [\Sigma[w(Fo^2 - Fc^2)^2]/\Sigma w(Fo^2)^2]^{1/2}$.

Table 2
Selected bond distances (Å) and angles (°) for azo dyes **1** and **2·CH$_3$COCH$_3$**

1	**LT (120 K)**	**1**	**RT (291 K)**
Bond distances		*Bond distances*	
O1–C2	1.230(3)	O1–C2	1.223(3)
N3–C1	1.322(3)	N3–C1	1.316(3)
C1–C2	1.474(3)	C1–C2	1.467(3)
N1–C2	1.381(3)	N1–C2	1.374(3)
N3–N4	1.323(3)	N3–N4	1.317(2)
O2–C3	1.220(3)	O2–C3	1.215(3)
N1–C3	1.396(3)	N1–C3	1.386(3)
N2–C8	1.140(4)	N2–C8	1.142(4)
N4–C10	1.407(3)	N4–C10	1.388(3)
N5–C11	1.458(3)	N5–C11	1.453(3)
C1–C5	1.444(3)	C1–C5	1.446(3)
C3–C4	1.463(4)	C3–C4	1.461(3)
C4–C5	1.355(3)	C4–C5	1.348(3)
Bond angles		*Bond angles*	
N4–N3–C1	119.8(2)	N4–N3–C1	120.1(2)
N3–N4–C10	118.1(2)	N3–N4–C10	118.8(2)
N2–C8–C4	177.8(3)	N2–C8–C4	177.6(3)
2·CH$_3$COCH$_3$; for two sets of data, RT (291 K)			
Bond distances		*Bond distances*	
O1–C2	1.213(7)	O5–C17	1.210(5)
N3–C1	1.314(5)	N8–C16	1.317(5)
C1–C2	1.469(8)	C16–C17	1.472(6)
N1–C2	1.363(7)	N6–C17	1.375(5)
N3–N4	1.316(5)	N8–N9	1.312(5)
O2–C3	1.216(7)	O6–C18	1.212(5)
N1–C3	1.384(7)	N6–C18	1.390(5)
N2–C8	1.119(6)	N7–C23	1.131(6)
N4–C10	1.389(5)	N9–C25	1.386(5)
C1–C5	1.446(6)	C16–C20	1.442(6)
C3–C4	1.448(8)	C18–C19	1.458(6)
C4–C5	1.339(6)	C19–C20	1.347(6)
C13–Cl1	1.736(5)	C28–Cl3	1.725(4)
Bond angles		*Bond angles*	
N4–N3–C1	119.4(4)	N9–N8–C16	120.3(4)
N3–N4–C10	119.1(4)	N8–N9–C25	118.5(3)
N2–C8–C4	178.8(4)	N7–C23–C19	178.5(4)

components, **1** and **2** exist in the hydrazone form both at 120 and 291 K, which can also be evidenced by the bond lengths of related atoms. The bond lengths of O1–C2 and N3–C1 in **1** are 1.230(3) and 1.322(3) Å at 120 K and 1.223(3) and 1.316(3) Å at 291 K, while those of O1–C2, N3–C1 and O5–C17, N8–C16 in **2** are in the range of 1.210(5)–1.317(5) Å at 291 K, indicative of partial double-bond character. In contrast, the bond lengths of C1–C2, N1–C2 and N3–N4 in **1** are in the ranges of 1.323(3)–1.474(3) Å at 120 K and 1.317(3)–1.467(3) Å at 291 K, while those of C1–C2, N1–C2, N3–N4 and C16–C17, N6–C17, N8–N9 in **2·CH$_3$COCH$_3$** are in the ranges of 1.316(5)–1.469(8) Å and 1.312(5)–1.472(6) Å at 291 K, respectively, exhibiting predominantly single-bond character (Table 2). These data are analogous to those previously reported four structures.

By comparing the two structures, it is found that a subtle change of the substituted group (with and without the chlorine substituted phenyl ring) in the backbone results in different dihedral angles between the pyridine-2,6-dione ring and the phenyl ring at each side of azo unit and different packing modes. The dihedral angles between two aromatic rings in the molecular structures of **1** and **2·CH$_3$COCH$_3$** are 16.2(2)° in **1** and 4.6(3)° and 1.3(3)° in **2·CH$_3$COCH$_3$**. There are two sets of molecules in the packing structure of **1** with the mean dihedral angle of 17.4(2)°, while all the molecules in **2·CH$_3$COCH$_3$** are packed in a parallel way. Typical π–π stacking interactions are observed in **1** between one pyridine-2,6-dione ring and another adjacent phenyl ring, forming a dimeric structure with the centroid–centroid separation of 3.658(3) Å and the dihedral angle of 2.1(2)°. However, as illustrated in Fig. 3, the centroid–centroid separation between the dimeric units is much longer with the centroid–centroid separation of 4.660(3) Å and the dihedral angle of 19.8(2)°, indicative of no π–π stacking interactions between them. The mean interlayer separation between molecules in the packing structure of **1** is as short as 3.002(3) Å, as can be seen in Fig. 4. In contrast, no π–π stacking interactions can be observed in the packing structure of **2·CH$_3$COCH$_3$** because the centroid–centroid separations between different types of aromatic rings are 4.578(6), 4.823(6), 5.014(6), and 5.037(6) Å. Nevertheless, a layer packing structure is also constituted with the mean interlayer contacts of 3.316(6) Å although all the aromatic rings are positioned in an offset way (Fig. 5).

It is worthwhile to mention that strong intramolecular N–H···O and weak intermolecular C–H···O hydrogen bonding interactions are found in **1** and **2·CH$_3$COCH$_3$**. The nitro group in **1** and **2·CH$_3$COCH$_3$** is fixed on the same side of N–H group where two adjacent six-membered hydrogen-bonded rings are formed. The donor is the hydrogen atom of N–H group and the acceptors are atoms O1 and O3 from two aromatic rings (Table 3). It is suggested that the formation of these intramolecular N–H···O hydrogen bonds should

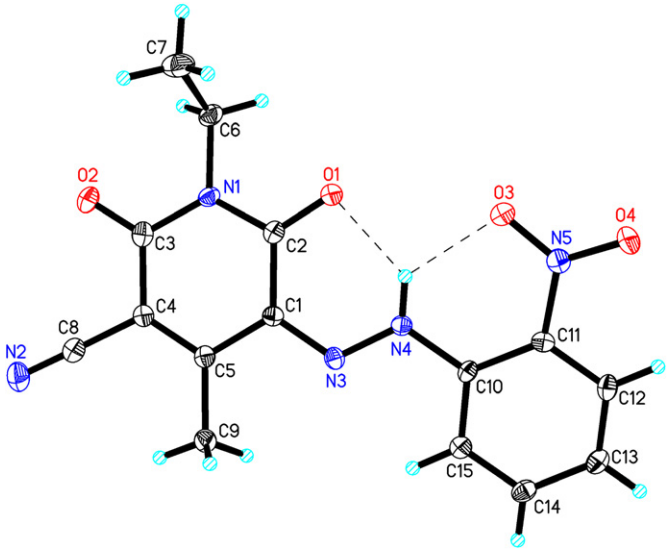

Fig. 1. An ORTEP drawing of compound **1**, with the atom-numbering scheme. Displacement ellipsoids are drawn at the 30% probability level and the H atoms are shown as small spheres of arbitrary radii.

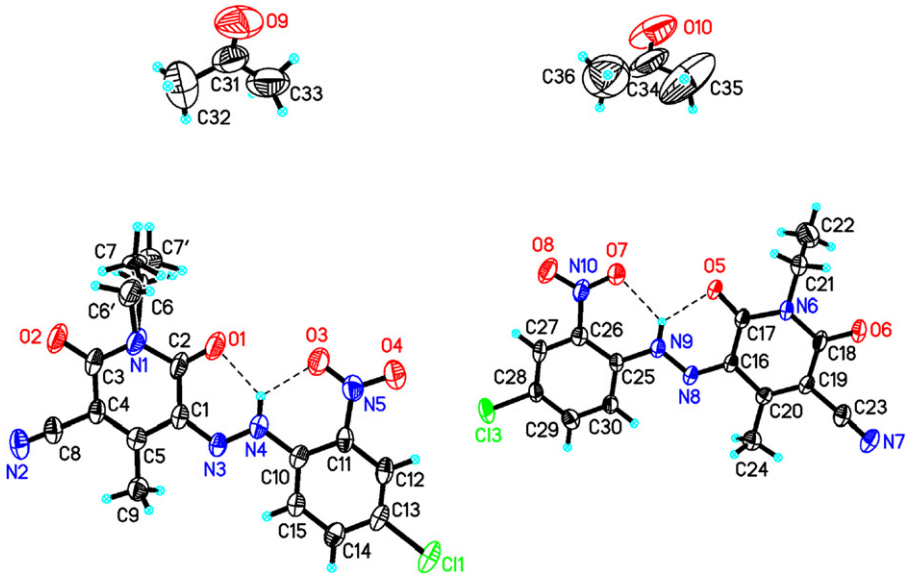

Fig. 2. An ORTEP drawing of compound **2**·CH_3COCH_3, with the atom-numbering scheme. Displacement ellipsoids are drawn at the 30% probability level and the H atoms are shown as small spheres of arbitrary radii.

contribute to stabilizing the hydrazone form in the solid state. In addition, intermolecular C—H···O hydrogen bonding is present between one hydrogen atom of the phenyl ring (C13) and one oxygen atom (O3) of the nitro group in **1** (Fig. 6), and different hydrogen atoms of the phenyl ring (C15 and C29) and the oxygen atoms of solvent acetone molecules (O9 and O10).

Actually the names of this kind of azo dyes are given according to the 2-hydroxy-6-pyridone isomer in most of the references. However, it is suggested to name them by the pyridine-2,6-dione form in order to be consistent with their solid structures. For example, in this work, C.I. Disperse Yellow 119 can be better named as nitrophenyl-2-[(1-ethyl-5-cyano-4-methyl-2,6-dioxo-1,2,3,6-tetrahydropyridin-3-ylidene)-hydrazino]benzoate rather than 5-(2-nitrophenyl)-azo-6-hydroxy-1-ethyl-3-cyano-4-methyl-2-pyridone, and C.I. Disperse Yellow 211 can be better named as 5-chloro-1-nitrophenyl-2-[(1-ethyl-5-cyano-4-methyl-2,6-dioxo-1,2,3,6-tetrahydropyridin-3-ylidene)-hydrazino]benzoate instead of 5-(4-chloro-2-nitrophenyl)-azo-6-hydroxy-1-ethyl-3-cyano-4-methyl-2-pyridone.

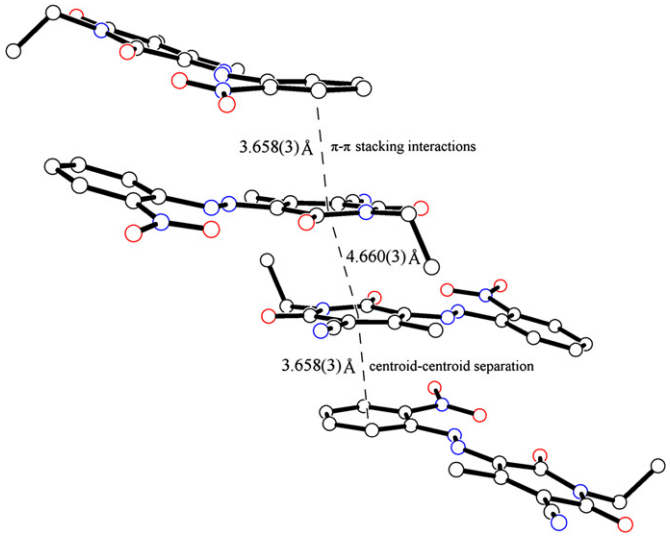

Fig. 3. A perspective view of the dimeric stacking between different types of aromatic rings in **1** where the centroid—centroid separations are shown. The hydrogen atoms are omitted for clarity.

3.2. Quantum chemical calculations

All the Density Function Theory (DFT) computations are carried out with the Gaussian 03, Revision C.02 programs [18] using the MPW1PW91 method and the LanL2DZ basis set. The fixed atom coordinates of **1** and **2**, originating from the structural parameters determined by the X-ray diffraction method, are used as the input file for the total energy calculation.

DFT calculations are carried out to compare the energy differences between the single-crystal structures and energy-minimized structures for both pyridine-2,6-dione and

Table 3
Hydrogen bonding interactions (Å, °) in compounds **1** and **2**·CH_3COCH_3

D—H···A	D—H	H···A	D···A	∠DHA	Symmetry code
1					
N4—H4···O1	0.86	1.93	2.582(3)	132.0	
N4—H4···O3	0.86	2.00	2.614(3)	127.0	
C13—H13···O3	0.93	2.50	3.329(3)	149.0	$1/2+x$, y, $1/2-z$
2·CH_3COCH_3					
N4—H4···O1	0.86	1.87	2.543(5)	133.0	
N4—H4···O3	0.86	2.00	2.608(5)	127.0	
N9—H9···O5	0.86	1.93	2.590(5)	132.0	
N9—H9···O7	0.86	2.01	2.619(5)	127.0	
C15—H15···O9	0.93	2.56	3.384(8)	148.0	x, $-1+y$, z
C29—H29···O10	0.93	2.41	3.175(10)	139.0	x, $-1+y$, z

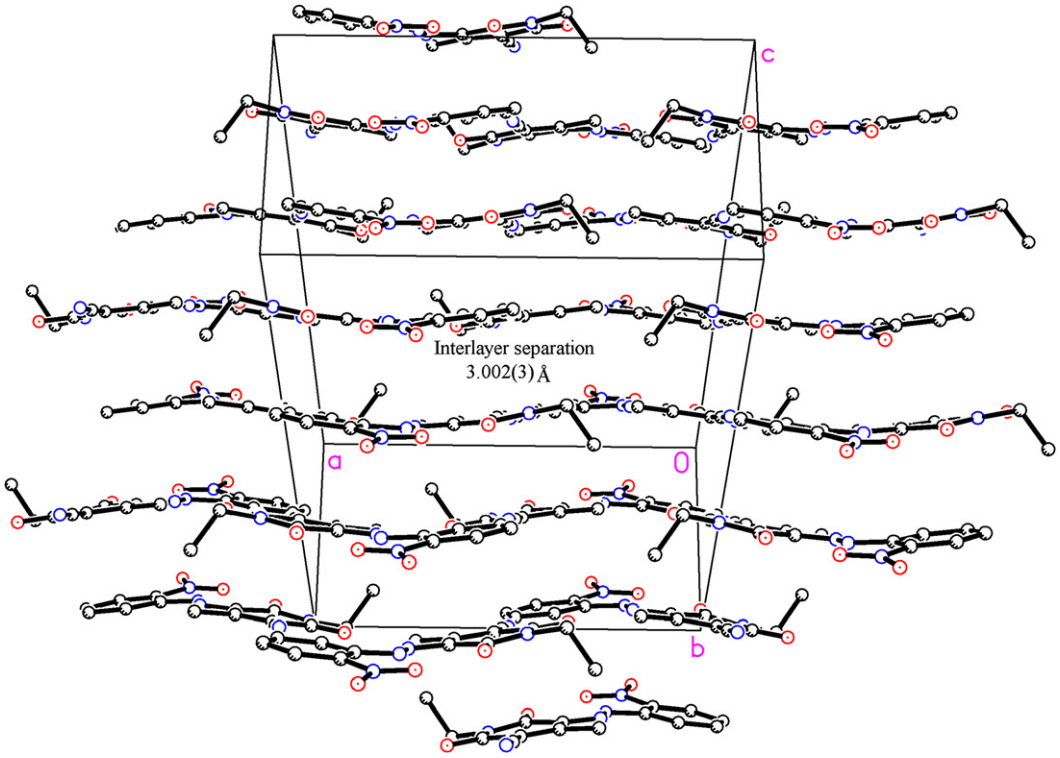

Fig. 4. A perspective view of the interlayer stacking in **1** together with the unit cell. The hydrogen atoms are omitted for clarity.

2-hydroxy-6-pyridone isomers of **1** and **2**. The total energy and the dipole moments for the single-crystal structures of **1** and **2** are −3,024,979.5 kJ/mol, 2.6×10^{-29} C m and −3,062,610.5 kJ/mol, 1.7×10^{-29} C m, respectively, while the ground state optimization for the pyridine-2,6-dione isomers, which are the same as the solid structure of **1** and **2**, gives the energy and the dipole moments of −3,025,618.4 kJ/mol, 2.6×10^{-29} C m and −3,063,247.9 kJ/mol, 1.7×10^{-29} C m, respectively. In contrast, the ground state optimization for the 2-hydroxy-6-pyridone isomers of **1** and **2** gives the higher energy of −3,025,450.3 and −3,063,082.1 kJ/mol and lower dipole moments of 1.9×10^{-29} and 1.5×10^{-29} C m.

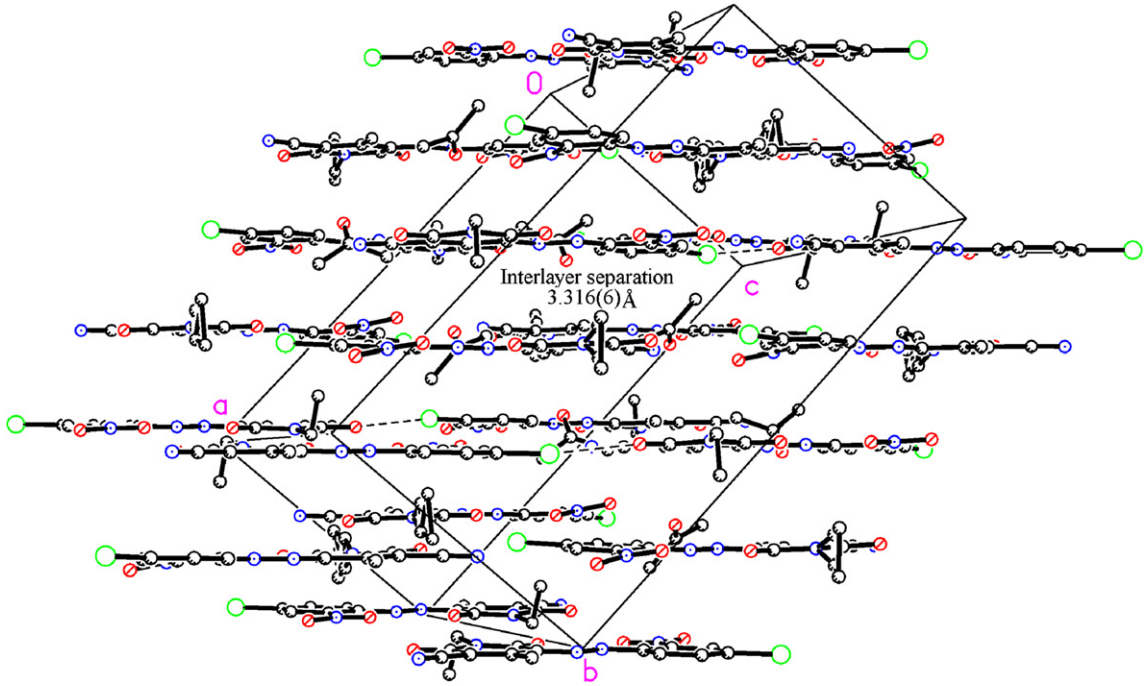

Fig. 5. A perspective view of the interlayer stacking in **2**·CH_3COCH_3 together with the unit cell. The hydrogen atoms are omitted for clarity.

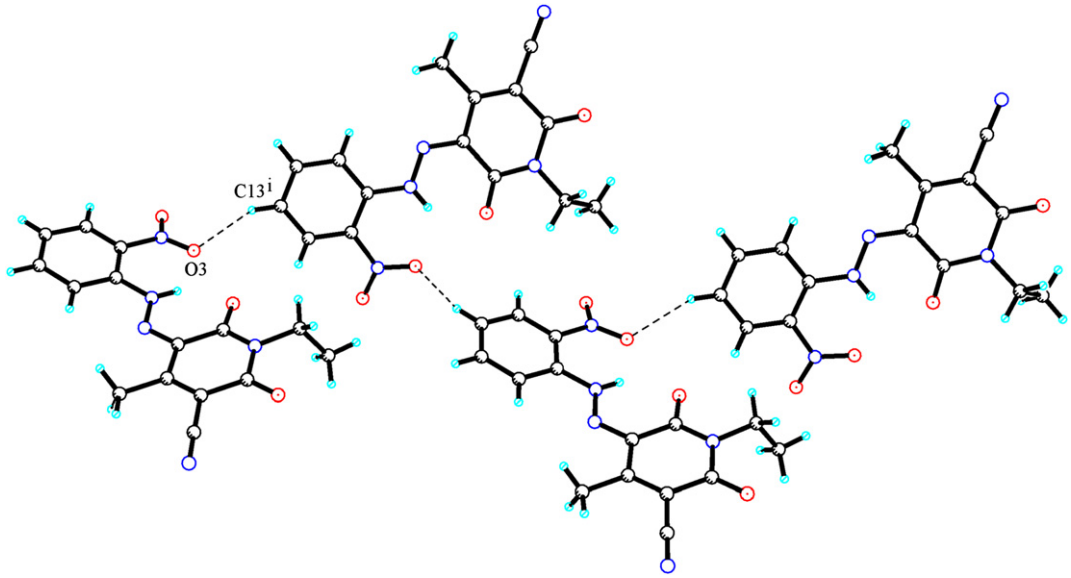

Fig. 6. A perspective view of the hydrogen-bond contacts in **1**. Hydrogen bonds are indicated as dashed lines and the labels are given only once for clarity. Translation of symmetry code to the equivalent positions: (i) $1/2 + x$, y, $1/2 - z$.

The results demonstrate large energy gaps between the single-crystal structures and energy-minimized structures in the same hydrazone form (638.9 and 637.4 kJ/mol for **1** and **2**), which may be the reflection of the energy compensation of the formation of hydrogen bonding and π–π stacking between molecules. They also indicate that the pyridine-2,6-dione isomer is somewhat more thermally stable than the 2-hydroxy-6-pyridone isomer for **1** and **2** with the energy gaps of 168.1 and 165.8 kJ/mol, which may be regarded as theoretical supports for the crystallization in the hydrazone form for **1** and **2**.

In Table 4, we summarize the computational details of four azo dyes (C.I. Disperse Yellow 114, 119, 126 and 211) where the data of C.I. Disperse Yellow 114 are adopted from one of our previously published papers [11]. They all show the same afore-mentioned tendency which can be known by the energy differences between the single-crystal and energy-minimized structures and those between the energy-minimized pyridine-2,6-dione and 2-hydroxy-6-pyridone isomers. Here one can draw the conclusion that both experimental and theoretical studies demonstrate the existence in the hydrazone form for this family of azo dyes in the solid state, which can be further stabilized by single or multiple six-membered intramolecular hydrogen-bonded rings.

4. Conclusion

X-ray single-crystal diffraction studies for C.I. Disperse Yellow 119 and C.I. Disperse Yellow 211 are described in this paper. Both azo dyes crystallize in the hydrazone form both at 291 and 120 K, but different dihedral angles between the pyridine-2,6-dione ring and the phenyl ring at each side of azo unit and different packing modes are observed due to the subtle change of the substituted group (with and without the chlorine atom) in the backbone. Two adjacent six-membered intramolecular hydrogen-bonded rings as well as intermolecular π–π stacking interactions are responsible for forming planar molecular structures and layer packing frameworks in **1** and **2**·$\mathbf{CH_3COCH_3}$. Furthermore, for four azo dyes which have been structurally elucidated by our group (C.I. Disperse Yellow 114, 119, 126 and 211), systematic comparisons of DFT calculations are performed on the energy

Table 4
Computational details for four azo dyes having the same pyridine-2,6-dione backbone (the total energy in kJ/mol and the dipole moment in C m)

Compounds	C.I. Disperse Yellow 114 [11]	C.I. Disperse Yellow 119 (**1**)	C.I. Disperse Yellow 126	C.I. Disperse Yellow 211 (**2**)
Calculation methods/basis set	DFT/MPW1PW91/LanL2DZ			
Energy/dipole moment (derived from the *single-crystal structures* in the hydrazone form)	$-3{,}608{,}767.2/3.8 \times 10^{-29}$	$-3{,}024{,}979.5/2.6 \times 10^{-29}$	$-3{,}891{,}007.6/3.3 \times 10^{-29}$	$-3{,}062{,}610.5/1.7 \times 10^{-29}$
Energy/dipole moment (derived from the *energy-minimized structures* in the pyridine-2,6-dione form)	$-3{,}609{,}880.7/3.8 \times 10^{-29}$	$-3{,}025{,}618.4/2.6 \times 10^{-29}$	$-3{,}893{,}616.8/3.1 \times 10^{-29}$	$-3{,}063{,}247.9/1.7 \times 10^{-29}$
Energy/dipole moment (derived from the *energy-minimized structures* in the 2-hydroxy-6-pyridone form)	$-3{,}609{,}727.2/2.6 \times 10^{-29}$	$-3{,}025{,}450.3/1.9 \times 10^{-29}$	$-3{,}893{,}458.9/3.5 \times 10^{-29}$	$-3{,}063{,}082.1/1.5 \times 10^{-29}$

differences between the single-crystal and energy-minimized structures and those between the energy-minimized pyridine-2,6-dione and 2-hydroxy-6-pyridone isomers. It is concluded that both experimental and theoretical studies support the formation of the hydrazone form for this family of azo dyes in the solid state both at 291 and 120 K.

Acknowledgements

The author would like to acknowledge the Major State Basic Research Development Programs (No. 2007CB 925101 and No. 2006CB806104), the National Natural Science Foundation of China (No. 20301009 and No. 20721002) and the Scientific Research Foundation for the Returned Overseas Chinese Scholars, State Education Ministry for financial aid.

Appendix. Supplementary material

CCDC reference numbers 656424 and 656425 for **1** at 120(2) K and **2**·**(CH_3COCH_3)** at 291(2) K contain the supplementary crystallographic data for this paper. These data can be obtained free of charge at www.ccdc.cam.ac.uk/conts/retrieving.html [or from the Cambridge Crystallographic Data Centre, 12, Union Road, Cambridge CB2 1EZ, UK; fax: (internat.) +44 1223/336 033; e-mail: deposit@ccdc.cam.ac.uk]. In addition, the CIF of **1** at 291(2) K is also attached for reference. Supplementary data associated with this article can be found in the online version, at doi:10.1016/j.dyepig.2008.01.007.

References

[1] Prikryl J, Burgert L, Halama A, Kralovsky J, Akrman J. Dyes Pigments 1994;26:107.
[2] Tsatsaroni EG, Kehayoglou AH, Eleftheriadis IC, Kyriazis LE. Dyes Pigments 1998;38:65. and references therein.
[3] Guzel B, Akgerman A. J Supercrit Fluid 2000;18:247.
[4] Chung YS, Son EJ, Lee KW. Text Res J 2001;71:174.
[5] Kim M, Yoon S, Kim T, Bae JS, Yoon N. Fiber Polym 2006;7:352.
[6] Sahin S, Demir C, Gucer S. Dyes Pigments 2007;73:368.
[7] Lee JJ, Han NK, Lee WJ, Choi JH, Kim JP. Color Technol 2002;118:154.
[8] Chung YS. Text Res J 2000;70:550.
[9] Schmidt A, Bach E, Schollmeyer E. Dyes Pigments 2003;56:27.
[10] Jenkins DW, El-Tahlawy K, El-Shafei A, Freeman HS, Hudson SM. Color Technol 2006;122:345.
[11] Huang W, Qian HF. Dyes Pigments 2008;77:446.
[12] Qian HF, Huang W. Acta Crystallogr Sect C 2006;62:o62.
[13] SMART and SAINT. Area detector control and integration software. Madison, Wisconsin (USA): Siemens Analytical X-ray Systems, Inc.; 2000.
[14] Sheldrick GM. SADABS, program for empirical absorption correction of area dectector data. Germany: University of Gottingen; 2001.
[15] Sheldrick GM. SHELXTL (version 6.10) software reference manual. Madison, Wisconsin (USA): Bruker AXS, Inc.; 2000.
[16] Black SN, Davey RJ, Slawin AMZ, Williams DJ. Acta Crystallogr Sect C 1992;48:323.
[17] Prikryl J, Kratochvil B, Ondracek J, Maixner J, Klicnar J, Huml K. Collect Czech Chem Commun 1993;58:2121.
[18] Frisch MJ, Trucks GW, Schlegel HB, Scuseria GE, Robb MA, Cheeseman JR, et al. Gaussian 03, revision C.02. Pittsburgh, PA: Gaussian, Inc.; 2004.